JACS
JOURNAL OF THE AMERICAN CHEMICAL SOCIETY

Article

pubs.acs.org/JACS

Biomimetic Preparation and Dual-Color Bioimaging of Fluorescent Silicon Nanoparticles

Sicong Wu, Yiling Zhong, Yanfeng Zhou, Bin Song, Binbin Chu, Xiaoyuan Ji, Yanyan Wu, Yuanyuan Su, and Yao He*

Jiangsu Key Laboratory for Carbon-Based Functional Materials and Devices, Institute of Functional Nano and Soft Materials (FUNSOM), Soochow University, Suzhou 215123, China

Supporting Information

ABSTRACT: Fluorescent silicon nanoparticles (SiNPs), as the most important zero-dimensional silicon nanostructures, hold high promise for long-awaited silicon-based optic applications. There currently remain major challenges for the green, inexpensive, and mass production of fluorescent SiNPs, resulting in difficulties in sufficiently exploiting the properties of these remarkable materials. Here, we show that fluorescent small-sized (~3.8 nm) SiNPs can be produced through biomimetic synthesis in rapid (10 min), low-cost, and environmentally benign manners. The as-prepared SiNPs simultaneously feature bright fluorescence (quantum yield (QY), ~15−20%), narrow emission spectral width (full width at half-maximum (fwhm), ~30 nm), and nontoxicity, making them as high-quality fluorescent probes for biological imaging in vitro and in vivo.

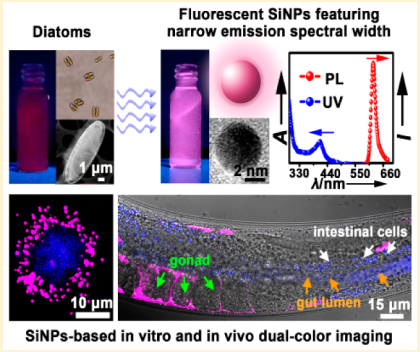

SiNPs-based in vitro and in vivo dual-color imaging

INTRODUCTION

Silicon, known as the second richest element in the earth (behind oxygen), is the leading element and dominates the current semiconductor industry. In the past decade, silicon nanotechnology has developed as one of the most important branches in the field of nanoscience, potentially revolutionizing silicon-related basic research and practical applications. Silicon functional nanomaterials are fundamental tools for promoting the advancement of silicon nanotechnology.[1] Among them, fluorescent silicon nanoparticles (SiNPs), as representative zero-dimensional silicon nanostructure, have shown great promise for various optic applications.[1f−j] Recent years have witnessed exciting progress in the production of fluorescent SiNPs,[2,3] including our latest achievement in the design of water-dispersed and highly luminescent SiNPs.[2] However, expensive, toxic, or flammable silicon resources (e.g., silicon wafer, organosilicone molecules, etc.) or additional chemical reagents (e.g., hydrofluoric/nitric acid, glutaric acid, etc.) are generally required as reaction precursor, which therefore hinders the facile availability of SiNPs and may lead to potential environmental contamination.[2] Moreover, despite strong fluorescence, most of the prepared fluorescent SiNPs feature relatively broad fwhm values (generally >70 nm).[2,3] As thus, there exists scanty information concerning SiNPs-based in vitro and in vivo multicolor imaging, limiting SiNPs-based wide-ranging applications in the bioimaging field.

On the other hand, diatoms, which widely exist in the Earth's wet and damp habitats, are known as a typical kind of single-celled plant. They are unicellular algae with a hallmark intricate siliceous cell wall composed of two valves that fit together like the two halves of a Petri dish. Moreover, diatoms contains sufficient silicon element that exists in the forms of silicate, silicic acid, and porous amorphous silica.[4] Significantly, taking advantages of their unique merits (e.g., silica framework with controlled morphologies, photonic crystal properties, complex quasi-periodic mechanical structure, etc.), diatoms have been extensively exploited as one of the most important subjects for biomimetic applications, including fabrication of three-dimensional photonic devices, construction of natural optical sensor, design of controllable assembly structures, etc.[5] Of our particular interest, the approximate μm level of diatoms is a suitable scale for nanostructure production. For example, Sandhage and co-workers converted diatoms into co-continuous and nanocrystalline silicon replicas, which were efficacious for gas-sensing applications, by reaction with magnesium gas through a magnesiothermic reduction process at 650 °C.[5a]

Inspired by these studies, we present a novel biomimetic strategy for the preparation of fluorescent SiNPs with a production yield of ~40% in facile, rapid, cheap, and green manners. Significantly, small-sized (diameter, ~3.8 nm) and fluorescent (QY, ~15−20%) SiNPs with high crystallization can be readily formed in 10 min of microwave irradiation by using diatoms as accessible and nontoxic silicon precursor, without requirement of any other additional chemical reagents. Of particular note, in addition to strong fluorescence and favorable biocompatibility, the SiNPs exhibit extremely narrow emission spectral width, with a notably low fwhm value of ~30 nm, enabling feasibility of dual-color bioimaging in vitro and in vivo.

Received: August 17, 2015
Published: October 28, 2015

DOI: 10.1021/jacs.5b08685
J. Am. Chem. Soc. 2015, 137, 14726−14732

RESULTS AND DISCUSSION

The biomimetic synthetic strategy is schematically illustrated in Figure 1a. Typically, elliptical-shaped Hantzschia amphioxys,

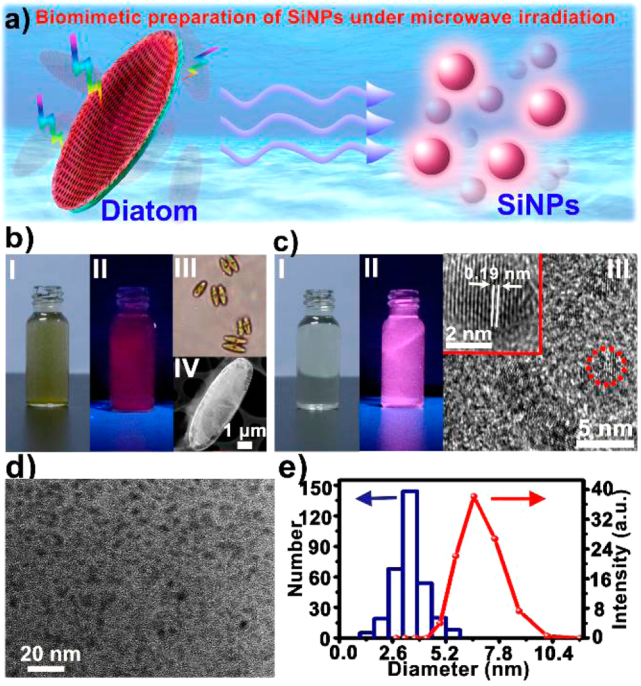

Figure 1. (a) Schematic illustration of biomimetic synthesis of SiNPs. (b) I and II indicate the diatom precursor solution under ambient light (left) and 365 nm irradiation (right), respectively; III and IV present microscope photo and TEM image of the diatoms, respectively. (c) I and II indicate as-prepared SiNPs sample solution under ambient light (left) and 365 nm irradiation (right), respectively; III shows HRTEM image of SiNPs with high crystallinity. Inset in (III) presents the enlarged HRTEM image of a single SiNP. (d) TEM images of the as-prepared SiNPs. (e) TEM diameter distribution and the DLS spectrum of the SiNPs.

recognized as one typical kind of diatom, are employed as environmentally friendly silicon resources in our experiment. As shown in Figure 1b (I and II), the aqueous solution dispersed with the diatoms is obviously turbid and exhibits faint, dark-red light under UV irradiation, which is due to luminescence of chlorophyll that exists in the diatoms.[6] Moreover, on the basis of morphology characterizations of optical microscope and transmission electronic microscopy (TEM), this kind of diatom features an amorphous structure with approximately μm level in sizes (~10−30 μm in length and ~2−3 μm in diameter, as shown in Figure 1b (III and IV) and Figure S1). Strikingly, after 10 min of microwave treatment, such large-size diatoms are transformed into ultrasmall SiNPs (~3.8 nm in diameter) with high crystallinity (Figure 1c (III)). More importantly, the resultant SiNPs sample solution is completely transparent in ambient environment and produces strong pink luminescence under UV irradiation, indicating excellent aqueous dispersibility and high fluorescence of the resultant SiNPs (Figure 1c (I and II)). The prepared SiNPs with spherical structures possess good monodispersity (Figure 1d), with the well-resolved (220) lattice planes of ~0.19 nm spacing in the high-resolution TEM (HRTEM) image (obtained as an average over 5 measurements to reduce the error to 5%),[7] demonstrating excellent crystallinity of the resultant SiNPs. The diameter distribution in Figure 1e, determined through the measurement of over 250 particles in the TEM image, displays an average size of 3.8 ± 0.8 nm, a bit smaller (~6.50 nm) than that determined by dynamic light scattering (DLS), which is due to distinct surface states of the SiNPs samples under the different measurement environments.[2] The energy-dispersive X-ray (EDX) pattern further qualitatively demonstrates the existence of Si and O in the SiNPs (Figure S2). It is worthwhile to note that microwave dielectric heating is of essential importance to take advantage of several unique merits of microwave irradiation.[2c,8] In our experiment, the diatom is heated under the same reaction temperature and time through electric heating jacket as a control. The resultant product shows amorphous and ambiguous structures with feeble fluorescence (Figure S3), which is in sharp contrast to the high crystallinity and strong fluorescence of the SiNPs prepared via microwave irradiation (Figure 1). In addition, other types of diatoms (e.g., Nitzschia sp., Melosira varians, Chaetoceros muelleri, etc.), serving as reaction precursor, are also efficacious for the production of fluorescent SiNPs, whose optical properties are similar to those of SiNPs prepared via Hantzschia amphioxys, implying versatility of this presented biomimetic synthetic strategy (Figures S4−S6).

The "like dissolves like" theory is further employed for differentiating the red fluorescence of as-prepared SiNPs and chlorophyll naturally contained in diatoms.[9] In our case, chloroform, known as a classic type of organic solvent with hydrophobic property, is first mixed with water. Compared to that of chloroform (1.5 g/cm^3), water with lower density (1 g/cm^3) is located in the upper layer. Upon addition of the prepared SiNPs in the mixture, the SiNPs featuring hydrophilic property are well dispersed in water, which is due to their similar polarity. As a result, the upper layer shows distinct pink fluorescence of the SiNPs (the left bottle in Figure 2a). When the chlorophyll extracted from the diatoms is dispersed in the mixture instead, dark-red fluorescence of the chlorophyll is observed in the lower layer, which is owing to similar polarities

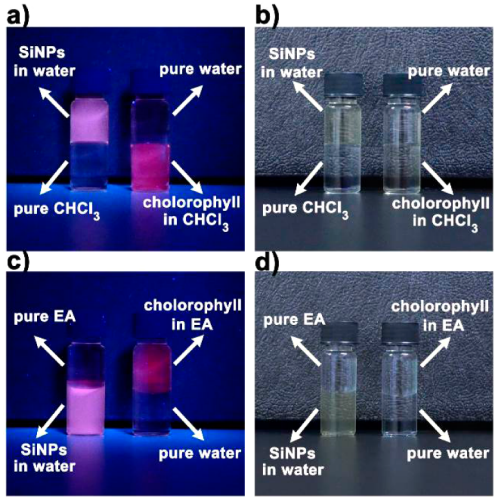

Figure 2. Hydrophilic property of the SiNPs. (a and b) Photographs of the water and chloroform mixture dispersed with the as-prepared SiNPs (left) or chlorophyll extracted from diatom (right) under 365 nm irradiation or ambient light. (c and d) Photographs of the water and ethyl acetate (EA) mixture dispersed with the as-prepared SiNPs (left) or chlorophyll extracted from diatom (right) under 365 nm irradiation or ambient light.

DOI: 10.1021/jacs.5b08685
J. Am. Chem. Soc. 2015, 137, 14726−14732

between the chlorophyll and chloroform (the right bottle in Figure 2a). To further confirm the result, ethyl acetate (EA), whose density (0.9 g/cm^3) is lower than that of water (1 g/cm^3), is also utilized as another typical kind of hydrophobic organic solvent for phase-separation investigation. Again, according to the "like dissolves like" theory, the as-prepared SiNPs are well dispersed in the water phase owing to their similar polarities, exhibiting strong pink fluorescence in the lower layer (the left bottle in Figure 2c). Instead, the chlorophyll with dark-red fluorescence is located in the upper layer, because its polarity is similar to that of EA (the right bottle in Figure 2c). Parts b and d of Figure 2 display the corresponding photographs imaged under the ambient environment, showing obvious stratification, and the as-prepared SiNPs are well dispersed in water due to their excellent aqueous dispersibility. These results provide further demonstration of pink fluorescence and hydrophilic property of the SiNPs.

Systematic characterizations including powder X-ray diffraction (XRD), high-resolution X-ray photoelectron spectroscopy (XPS), photoluminescence (PL) decay curves, and Fourier-transform infrared (FTIR) spectroscopy are further performed to investigate the physical/chemical features of the resultant SiNPs in a detailed way. As shown in Figure 3a, the

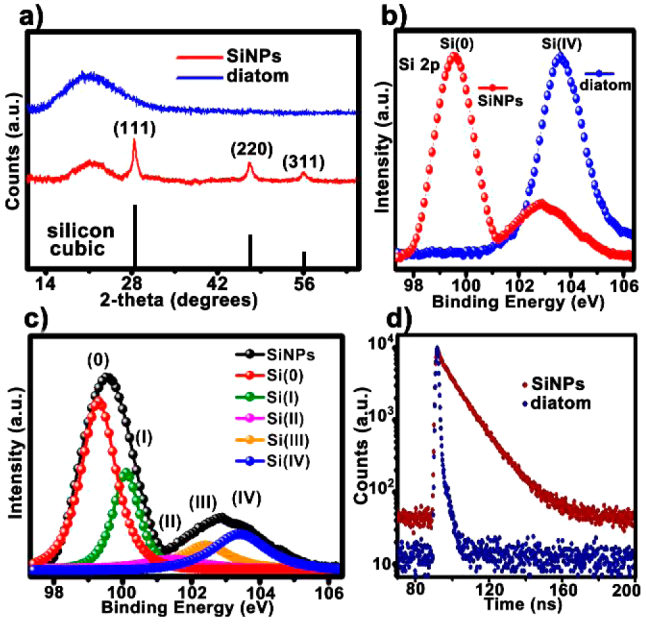

Figure 3. Systematic characterizations of the resultant SiNPs. (a) XRD spectra of the as-prepared SiNPs (red trace) and the pure diatoms (blue trace). (b) XPS of the as-prepared SiNPs (red trace) and the pure diatoms (blue trace) deposited on an indium tin oxide (ITO) conducting glass. (c) For clarity, only spectra with Si $2p_{3/2}$ signal are exhibited. (d) PL decay curves of the as-prepared SiNPs (dark-red trace) and the pure diatoms (dark-blue trace).

SiNPs exhibit three standard diffraction peaks at 28.4° (111), 47.3° (220), and 56.1° (311), while the pure diatoms show a broad unassigned diffraction peak arising from the amorphous SiO_2-like matrix.[10] Taken together with TEM/HRTEM results revealing the ultrasmall size of SiNPs (diameter, ~3.8 nm), we deduce the quantum confinement effects and high crystallization as two significant contributors to the observed pink fluorescence, well supported by previous reports.[11] The XPS spectrum of the SiNPs shows two peaks at ~99 and ~103 eV (Figure 3b), readily assigned to zerovalent silicon and oxides of silicon, implying a silica "skin" on the prepared SiNPs.[10] The oxidation state(s) of the SiNPs was further evaluated, as shown in Figure 3c. An intense emission at 99.3 eV ascribed to Si(0) was detected, while other peaks located at 100.3, 101.3, 102.4, and 103.4 eV were attributed to Si suboxides. Accordingly, the ratio value of Si(0)/Si(IV) is determined to be as high as 3.46:1.[12] In contrast, the XPS spectrum of the pure diatoms exhibits only one peak at ~103 eV, attributed to oxides of silicon. These XPS data suggest that Si(IV) contained in diatom precursor can be largely reduced to Si(0) that exists in the as-prepared SiNPs by the microwave irradiation.

PL decay measurement of both diatom and SiNPs is also employed, as displayed in Figure 3d. Typically, the PL decay curve of SiNPs is well fit to a second-order exponential decay. The decay times of the fast and slow components are 1.4 and 10.9 ns, respectively, with a calculated average lifetime of 10.8 ns. As is well-known, the existence of surface states would lead to a long radiative lifetime (generally over 10 ns) because the carriers are prone to be trapped by the surface states, while the intrinsic core-state recombination facilitates the decrease of lifetime.[13a] In comparison, the PL decay curve of the diatoms also can be fit to a second-order exponential decay. However, the decay times of the fast and slow components are 433 ps and 2.7 ns, respectively, with a calculated average lifetime of 1.1 ns. The shorter lifetime is attributed to the conventional fluorescent chromophore of the chlorophyll molecule, while the longer lifetime is caused by the greater structural rigidity of the chlorophyll molecule.[13b] It is worth pointing out that previous studies have revealed that average lifetimes for most organic dyes are <5 ns.[1g,13b] In marked contrast, fluorescent nanoparticles (e.g., semiconducting quantum dots) feature longer average lifetime values, equal to or larger than 10 ns,[1g,13a] well consistent with the previously mentioned results (i.e., fluorescent SiNPs exhibit an average lifetime of 10.8 ns, much longer than that (1.1 ns) of pure diatoms). Moreover, FTIR (Figure S7) provides additional demonstration of excellent aqueous dispersibility of the as-prepared SiNPs. Previous studies have demonstrated that the nanoscale biosilica that exists in diatoms contains a large amount of silaffins (a typical kind of protein having amino acids).[4b,14] Therefore, the resultant SiNPs are naturally surface-covered with the carboxylic acid groups and amino groups without affecting the nanoparticle crystallization (please also see a proposed mechanism in detail in Supporting Information).

Remarkably, the as-prepared SiNPs feature ultranarrow emission spectra width, with a fwhm value of ~30 nm, which is the lowest value ever reported for the water-dispersed SiNPs. Figure 4 diaplays the normalized UV-PL spectra of the as-prepared SiNPs, showing a distinct absorption peak and an extremely narrow PL peak located at 410 and 620 nm (red lines), respectively. In comparison, the control group (i.e., the pure diatom sample) with ambiguous absorption peak exhibits maximum emission wavelength at 680 nm (blue lines), obviously red-shifted compared to that of the SiNPs. In addition, the UV-PL spectrum of another kind of previously reported blue-emitting SiNPs,[2c] prepared by using organo-silicon small molecules (e.g., (3-aminopropyl)trimethoxysilane, $C_6H_{17}NO_3Si$) as silicon resource, is also presented as a control in our study (organo-silicon-derived SiNPs, black line). Typically, the organo-silicon-derived SiNPs exhibit a relatively broad emission peak with a large fwhm value of ~100 nm, similar to those (70−150 nm) of SiNPs prepared using bulk

DOI: 10.1021/jacs.5b08685
J. Am. Chem. Soc. 2015, 137, 14726−14732

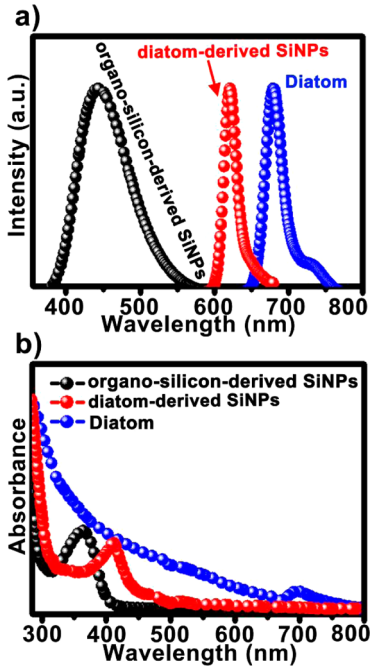

Figure 4. Optical properties of SiNPs. (a) Photoluminescence and (b) absorption spectra of the SiNPs prepared using organo-silicon molecules (organo-silicon-derived SiNPs, black lines) or diatom (diatom-derived SiNPs, red lines) as silicon precursor, as well as the pure diatoms (blue lines).

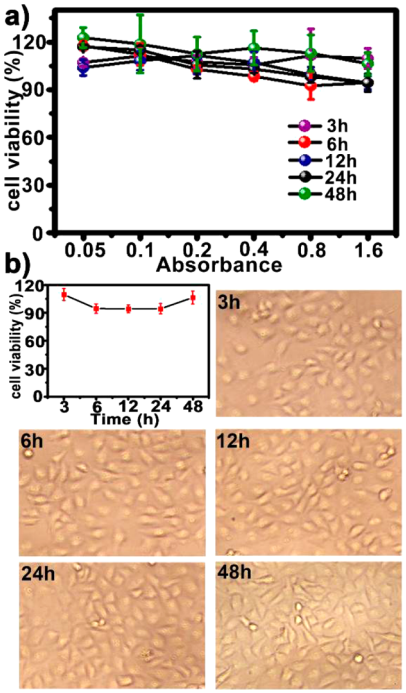

Figure 5. Cytotoxicity measurement of the resultant SiNPs. (a) Cytotoxicity of MCF-7 cells treated with the SiNPs of serial concentrations for different incubation times. (b) Cell viability and morphology of MCF-7 cells treated with the SiNPs, whose concentration is the same as that employed in the following bioimaging experiments for 3, 6, 12, 24, and 48 h, respectively.

silicon and silicon wafer as silicon precursor.[2,3] In marked contrast, our diatoms-derived SiNPs feature the lowest fwhm value ever reported, significantly down to ~30 nm. We deduce the narrow emission peak of diatoms as the dominant contributor to the observed low fwhm value of the prepared SiNPs (e.g., fwhm values of both diatoms and SiNPs are <50 nm). Besides, narrow size distribution and high monodispersibility of the prepared SiNPs (as mentioned in Figure 1d) are considered as additional factors, facilitating elimination of the effect of inhomogeneous broadening due to size fluctuations at room temperature.[15]

In addition to the unique optical properties, the resultant SiNPs have excellent biocompatibility due to non- or low toxicity of diatoms and silicon,[2c] producing negligible cytotoxicity during 48-h cellular incubation (Figure 5). Figure 5a exhibits that the cell viability of MCF-7 cells treated by the SiNPs preserves >90% at different concentrations (absorbance = 0.05−1.6) and incubation times (3−48 h), indicating SiNPs are non- or low-cytotoxic. Figure 5b shows that, during 48-h incubation, MCF-7 cells maintain normal morphology when treated by the SiNPs, whose concentration is the same as that utilized in the bioimaging studies, providing additional demonstration of feeble cytotoxicity of the as-prepared SiNPs. Moreover, the fluorescent SiNPs maintain relatively stable fluorescence in wide-ranging pH values and cellular environment (e.g., Dulbecco's modified Eagle's medium (DMEM) and RPMI-1640), offering the promising possibility for widespread biological applications (Figures S8 and S9).

The SiNPs containing surface-covered carboxylic acid and amino groups are easily conjugated with antibodies via well-studied *N*-(3-(dimethylamino)propyl)-*N*-ethylcarbodiimde hydrochloride (EDC)/*N*-hydroxysuccinimide (NHS) cross-linking reaction,[16] producing the SiNPs−protein bioprobes ready for immunological staining. In our experiment, of particular significance, we for the first time simultaneously employ the blue- and red-emitting SiNPs (both samples are prepared through the biomimetic synthesis, whose characterizations are shown in Figures 1 and S12) for dual-color immunofluorescent cellular imaging. Especially, the blue-emitting SiNPs probes are first targeted to the nucleus of Hela cells (a typical class of cervical cancer cells[17]), which are beforehand incubated with an antinucleus antibody. Afterward, a Hela cell whose nucleus is labeled by blue-emitting SiNPs is further blocked and incubated with monoclonal anti-α-tubulin. In the second step, the red-emitting SiNPs probes specifically target the microtubules of Hela cells through antibody−antigen immunoreactions. Such resultant SiNPs-labeled cells are finally captured by a laser-scanning confocal microscope (LSCM). As shown in Figure 6a and b, the nuclei and microtubules of Hela cells are obviously double-color imaged by the blue- and red-emitting SiNPs, respectively, with clearly spectral resolution. We further demonstrate feasibility of SiNPs-based dual-color bioimaging in vivo by using *C. elegans* as well-established animal models.[18] In our experiment, digestive and reproductive systems of *C. elegans* are microinjected with blue- and red-emitting SiNPs, respectively, followed with observation through confocal microscopy. As can be seen in Figure 6c, the bright fluorescent signal of blue-emitting SiNPs is easily visible in the gut lumen and intestinal cells of the injected worm. Meanwhile, distinct fluorescence that originated from red-emitting SiNPs also can be detected in the gonad of *C. elegans*, with high spectral and spatial resolution.

CONCLUSION

In conclusion, we mention the development of a new biomimetic strategy and starting materials as an alternative.

DOI: 10.1021/jacs.5b08685
J. Am. Chem. Soc. 2015, 137, 14726−14732

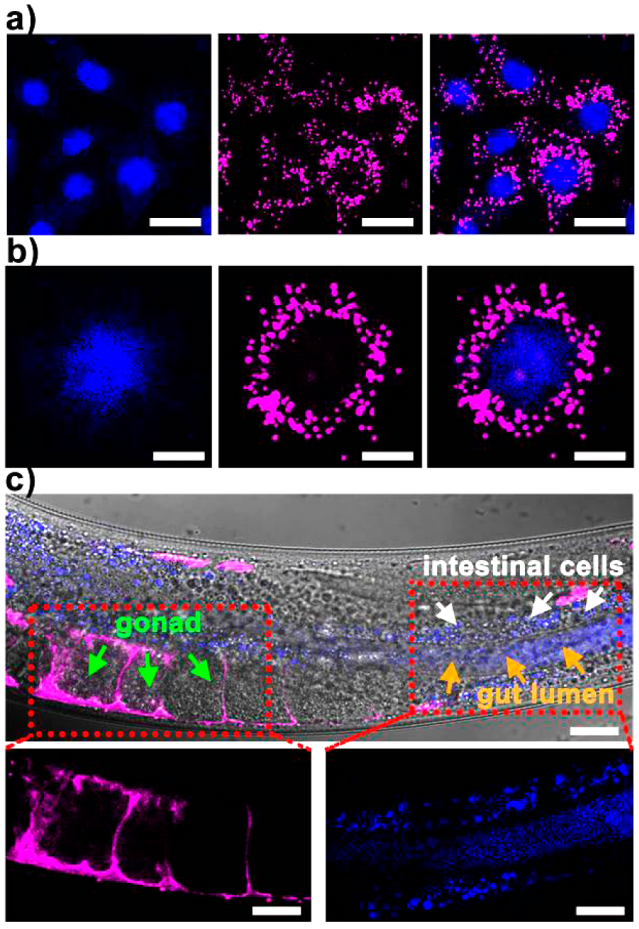

Figure 6. SiNPs-based dual-color bioimaging in vitro and in vivo. (a and b) Photos of dual-color immunofluorescent cell images captured by LSCM. ((left) nuclei are distinctively labeled by blue-emitting SiNPs; (middle) microtubules are distinctively labeled by red-emitting SiNPs; (right) superposition of the two fluorescence images. Scale bars of (a) are 20 μm. Scale bars of (b) are 10 μm.) (c) Representative confocal images of the as-prepared SiNPs in *C. elegans* by microinjection. The gonad (left) and gut lumen (right) are stained by blue- and red-emitting SiNPs, respectively (top). Bottom left and bottom right are enlarged views corresponding to the boxed areas in the top image; (top) scale bars = 20 μm; (bottom) scale bars = 15 μm.

The worldwide supply of natural diatoms has been estimated at >10 000 000 tonnes every year.[19] We have demonstrated that high-quality fluorescent SiNPs can be produced in facile, rapid, and green manners from diatoms, suggesting new promising opportunities for the creation of fluorescent SiNPs from accessible, green, and natural biomass precursors. Furthermore, taking advantage of the ultranarrow fwhm value (~30 nm) of the prepared SiNPs, we for the first time demonstrate feasibility of SiNPs-based dual-color bioimaging in vitro and in vivo. These results will pave the way for biomimetic preparation of fluorescent SiNPs, potentially facilitating the supply of functional silicon nanomaterials and advancement of SiNPs-based bioimaging field.[20]

EXPERIMENTAL METHODS

Synthesis of SiNPs. The samples of diatom were first separated through centrifugation at 6000 rpm for 10 min. The above steps were repeated three times to achieve the diatom free of impurity. The concentration of diatom was determined using a spectrophotometer by measuring the optical density (OD) at 420 nm absorbance.[21] For the preparation of SiNPs, 8 mL of diatom precursor solution with an OD value of 1 was added into the vitreous vessel. Afterward, the vessel was put into the microwave equipment and reacted under 150 °C/10 min to produce the SiNPs whose maximum emission is located at ~620 nm. After microwave irradiation and the temperature being reduced to 30 °C naturally, the SiNPs sample was removed and further filtrated by 0.22 μm filter membrane. In comparison to the precursor solution featuring feeble luminescence, the as-prepared SiNPs produce strong pink fluorescence when irradiated by UV lamp.

For purification, 10 kDa Nanosep was used for ultrafiltration to fully remove the impurities (e.g., organic matter and inorganic salts) in solution. The purified samples were then further used for our following experimental studies.

Note that the SiNPs with other luminescent colors and different sizes could be prepared through simply prolonging the reaction time. In our experiment, blue-emitting SiNPs with an average size of 2.1 ± 1.0 nm were readily obtained at 150 °C/180 min (see detailed characterizations in Figure S12). These resultant blue- and red-emitting SiNPs are then employed for dual-color bioimaging in vitro and in vivo in the following experiment.

MTT Assay of Cell Viability. Antibiotics (100 μg/mL streptomycin and 100 U/mL penicillin) and RPMI-1640 with 10% heat-inactivated fetal bovine serum (FBS), which served as cellular culture medium, were used for culturing human breast adenocarcinoma cells (MCF-7 cells) in the humidified atmosphere with 5% CO_2 at 37 °C and serial incubation times (e.g., 3, 6, 12, 24, and 48 h). The cytotoxicity of the SiNPs was determined through the MTT (3-(4,5-dimethylthiazol-2-yl)-2,5-diphenyltetrazolium bromide) assay (thiazolyl blue tetrazolium bromide (M5655)), well-recognized as an established assay means of cellular viability.[22]

pH Stability of SiNPs. HCl or NaOH was used for varying the pH of the SiNPs sample solution, monitored using Seven Multi pH meter (Mettler Toledo). Meanwhile, the HORIBA JOBIN YVON FLUOROMAX-4 spectrofluorimeter is utilized for recording the PL intensity of the SiNPs sample under different pH values. Moreover, we also investigated the pH stability of SiNPs in DMEM medium containing 10% fetal bovine serum (FBS) and RPMI-1640 medium containing 10% FBS.

Dual-Color Immunofluorescent Labeling Hela Cells Using the SiNPs/Antibody Conjugates. *N*-(3-(Dimethylamino)propyl)-*N*-ethylcarbodiimde hydrochloride (EDC) was used as zero-length cross-linkers for conjugating the amino groups of blue-emitting SiNPs with the carboxylic acid groups of the protein. In detail, 12.5 μL of goat antimouse IgG (4 mg/mL) is first mixed with 2 μL of EDC (6.4 mg/mL in H_2O), following by 15 min incubation at 25 °C to activate the carboxylic acid groups. The treated goat antimouse IgG was then incubated with 110 μL of blue-emitting SiNPs (in Milli-Q water, absorption value = 0.6, λ_{abs} = 410 nm) at 25 °C for 2 h of continuous shaking in the dark. The conjugation reaction was kept overnight at 4 °C. Afterward, centrifugation was performed to remove the isourea byproduct and residual reagent through 10 kDa Nanosep centrifugal devices at 5000 rpm for 15 min. The SiNPs/IgG conjugates that remained in the upper phase were then diluted using 30 μL of phosphate-buffered saline (PBS) (pH = 7.4, 0.1 M) buffer, finally producing the purified SiNPs/IgG conjugates, which were stored in the dark at 4 °C and used for the following bioimaging studies. For the preparation of the red-emitting SiNPs/antibody bioconjugates, the experimental procedures were identical to the above-mentioned manipulations.

For cellular imaging, antibiotics (100 μg/mL streptomycin and 100 U/mL penicillin) and DMEM with 10% heat-inactivated fetal bovine serum (FBS), which served as cellular culture medium, were first used for culturing Hela cells in the humidified atmosphere with 5% CO_2 at 37 °C overnight. After that, 4% sucrose and 4% paraformaldehyde were employed for fixing the Hela cells for 20 min, followed by 40 min blocking in PBS containing 4% BSA and 0.1% Triton X-100. PBS containing 0.1% Tween 20 was then utilized to wash the fixed Hela cells. For labeling nuclei, the resultant cells were first incubated with monoclonal anti-HN RNP for 1 h and then further treated with the blue-emitting SiNPs/IgG conjugates for another 1 h. Afterward, for

DOI: 10.1021/jacs.5b08685
J. Am. Chem. Soc. 2015, 137, 14726−14732

labeling microtubules, the treated cells were incubated with monoclonal anti-α-tubulin for 1 h, followed by the 1-h treatment of red-emitting SiNPs/IgG bioconjugates. Finally, the resultant samples were mounted on slides in fluoromount (Sigma, F4680) and captured by a confocal laser microscope (Leica, TCS-SP5). For both labeling nuclei and microtubules, diode laser ($\lambda_{excitation}$ = 405 nm, power = 50 mW) was used as the excitation light source. Detection windows for blue-emitting SiNPs and red-emitting SiNPs are 430−510 and 610−670 nm, respectively. For control experiments, the power of the diode laser ($\lambda_{excitation}$ = 405 nm) was the same. A cooled charge-coupled device (CCD) camera was used for capturing the confocal images at 15 s intervals, which were then analyzed through image analysis software.

***C. elegans* Maintenance and Microinjection.** The *C. elegans* of wild-type N2 Bristol was maintained on *Escherichia coli* OP50 seeded nematode growth media (NGM) plates at 20 °C. To double label different parts of *C. elegans*, blue-emitting SiNPs and red-emitting SiNPs were microinjected into the digestive system and the reproductive system of the same worm individually, and then the injected worms were examined with confocal laser microscope. The microinjection was performed by using Eppendorf Femtojet microinjector and NK2 transferman micromanipulator. In parallel, the analysis was also performed on the untreated worm as the control.

■ ASSOCIATED CONTENT

Ⓢ Supporting Information

The Supporting Information is available free of charge on the ACS Publications website at DOI: 10.1021/jacs.5b08685.

Materials and devices, PLQY measurements, additional data (Figures S1−S12), and corresponding discussions (PDF)

■ AUTHOR INFORMATION

Corresponding Author

*yaohe@suda.edu.cn

Author Contributions

S.W. and Y.Z. contributed equally.

Notes

The authors declare no competing financial interest.

■ ACKNOWLEDGMENTS

We thank Prof. Shuit-Tong Lee's general help and valuable suggestion. The authors appreciate financial support from National Basic Research Program of China (973 Program 2013CB934400, 2012CB932400), NSFC (61361160412, 31400860), and Projects Funded by the Priority Academic Program Development of Jiangsu Higher Education Institutions (PAPD), as well as Collaborative Innovation Center of Suzhou Nano Science and Technology (NANO-CIC).

■ REFERENCES

(1) (a) Patolsky, F.; Timko, B. P.; Yu, G. H.; Fang, Y.; Greytak, A. B.; Zheng, G. F.; Lieber, C. M. *Science* **2006**, *313*, 1100−1104. (b) Xie, P.; Xiong, Q. H.; Fang, Y.; Qing, Q.; Lieber, C. M. *Nat. Nanotechnol.* **2012**, *7*, 119−125. (c) Park, J. H.; Gu, L.; von Maltzahn, G.; Ruoslahti, E.; Bhatia, S. N.; Sailor, M. J. *Nat. Mater.* **2009**, *8*, 331−336. (d) Hochbaum, A. I.; Chen, R. K.; Delgado, R. D.; Liang, W. J.; Garnett, E. C.; Najarian, M.; Majumdar, A.; Yang, P. D. *Nature* **2008**, *451*, 163−167. (e) Dasgupta, N. P.; Liu, C.; Andrews, S.; Prinz, F. B.; Yang, P. D. *J. Am. Chem. Soc.* **2013**, *135*, 12932−12935. (f) Howes, P. D.; Chandrawati, R.; Stevens, M. M. *Science* **2014**, *346*, 1247390. (g) Cheng, X. Y.; Lowe, S. B.; Reece, P. J.; Gooding, J. J. *Chem. Soc. Rev.* **2014**, *43*, 2680−2700. (h) Peng, F.; Su, Y. Y.; Zhong, Y. L.; Fan, C. H.; Lee, S. T.; He, Y. *Acc. Chem. Res.* **2014**, *47*, 612−623. (i) McVey, B. F. P.; Tilley, R. D. *Acc. Chem. Res.* **2014**, *47*, 3045−3051. (j) Montalti, M.; Cantelli, A.; Battistelli, G. *Chem. Soc. Rev.* **2015**, *44*, 4853−4921. (k) Chiappini, C.; De Rosa, E.; Martinez, J. O.; Liu, X.; Steele, J.; Stevens, M. M.; Tasciotti, E. *Nat. Mater.* **2015**, *14*, 532−539.

(2) (a) He, Y.; Zhong, Y. L.; Peng, F.; Wei, X. P.; Su, Y. Y.; Lu, Y. M.; Su, S.; Gu, W.; Liao, L. S.; Lee, S. T. *J. Am. Chem. Soc.* **2011**, *133*, 14192−14195. (b) Zhong, Y. L.; Peng, F.; Wei, X. P.; Zhou, Y. F.; Wang, J.; Jiang, X. X.; Su, Y. Y.; Su, S.; Lee, S. T.; He, Y. *Angew. Chem., Int. Ed.* **2012**, *51*, 8485−8489. (c) Zhong, Y. L.; Peng, F.; Bao, F.; Wang, S. Y.; Ji, X. Y.; Yang, L.; Su, Y. Y.; Lee, S. T.; He, Y. *J. Am. Chem. Soc.* **2013**, *135*, 8350−8356. (d) Li, Q.; He, Y.; Chang, J.; Wang, L.; Chen, H. Z.; Tan, Y. W.; Wang, H. Y.; Shao, Z. Z. *J. Am. Chem. Soc.* **2013**, *135*, 14924−14927. (e) Zhong, Y. L.; Sun, X. T.; Wang, S. Y.; Peng, F.; Bao, F.; Su, Y. Y.; Li, Y. Y.; Lee, S. T.; He, Y. *ACS Nano* **2015**, *9*, 5958−5967.

(3) (a) Shiohara, A.; Hanada, S.; Prabakar, S.; Fujioka, K.; Lim, T. H.; Yamamoto, K.; Northcote, P.; Tilley, R. D. *J. Am. Chem. Soc.* **2010**, *132*, 248−253. (b) Zhang, X.; Brynda, M.; Britt, R. D.; Carroll, E. C.; Larsen, D. S.; Louie, A. Y.; Kauzlarich, S. M. *J. Am. Chem. Soc.* **2007**, *129*, 10668−10669. (c) Atkins, T. M.; Thibert, A.; Larsen, D. S.; Dey, S.; Browning, N. D.; Kauzlarich, S. M. *J. Am. Chem. Soc.* **2011**, *133*, 20664−20667. (d) Dasog, M.; Yang, Z. Y.; Regli, S.; Atkins, T. M.; Faramus, A.; Singh, M. P.; Muthuswamy, E.; Kauzlarich, S. M.; Tilley, R. D.; Veinot, J. G. C. *ACS Nano* **2013**, *7*, 2676−2685. (e) Dasog, M.; De los Reyes, G. B.; Titova, L. V.; Hegmann, F. A.; Veinot, J. G. C. *ACS Nano* **2014**, *8*, 9636−9648. (f) Sato, K.; Yokosuka, S.; Takigami, Y.; Hirakuri, K.; Fujioka, K.; Manome, Y.; Sukegawa, H.; Iwai, H.; Fukata, N. *J. Am. Chem. Soc.* **2011**, *133*, 18626−18633. (g) Erogbogbo, F.; Lin, T.; Tucciarone, P. M.; LaJoie, K. M.; Lai, L.; Patki, G. D.; Prasad, P. N.; Swihart, M. T. *Nano Lett.* **2013**, *13*, 451−456. (h) Qian, C. X.; Sun, W.; Wang, L. W.; Chen, C. L.; Liao, K.; Wang, W. D.; Jia, J.; Hatton, B. D.; Casillas, G.; Kurylowicz, M.; Yip, C. M.; Mastronardi, M. L.; Ozin, G. A. *J. Am. Chem. Soc.* **2014**, *136*, 15849−15852. (i) Zhou, T. L.; Anderson, R. T.; Li, H. S.; Bell, J.; Yang, Y. G.; Gorman, B. P.; Pylypenko, S.; Lusk, M. T.; Sellinger, A. *Nano Lett.* **2015**, *15*, 3657−3663.

(4) (a) Lang, Y.; del Monte, F.; Collins, L.; Rodriguez, B. J.; Thompson, K.; Dockery, P.; Finn, D. P.; Pandit, A. *Nat. Commun.* **2013**, *4*, 3683. (b) Grachev, M. A.; Annenkov, V. V.; Likhoshway, Y. V. *BioEssays* **2008**, *30*, 328−337. (c) Lettieri, S.; Setaro, A.; De Stefano, L.; De Stefano, M.; Maddalena, P. *Adv. Funct. Mater.* **2008**, *18*, 1257−1264.

(5) (a) Bao, Z. H.; Weatherspoon, M. R.; Shian, S.; Cai, Y.; Graham, P. D.; Allan, S. M.; Ahmad, G.; Dickerson, M. B.; Church, B. C.; Kang, Z. T.; Abernathy, H. W., III; Summers, C. J.; Liu, M.; Sandhage, K. H. *Nature* **2007**, *446*, 172−175. (b) Parker, A. R.; Townley, H. E. *Nat. Nanotechnol.* **2007**, *2*, 347−353. (c) Rosi, N. L.; Thaxton, C. S.; Mirkin, C. A. *Angew. Chem., Int. Ed.* **2004**, *43*, 5500−5503.

(6) (a) Kiefer, D. A. *Mar. Biol.* **1973**, *23*, 39−46. (b) Dutton, H. J.; Manning, W. M.; Duggar, B. M. *J. Phys. Chem.* **1943**, *47*, 308−313.

(7) Kiang, C. H.; Endo, M.; Ajayan, P. M.; Dresselhaus, G.; Dresselhaus, M. S. *Phys. Rev. Lett.* **1998**, *81*, 1869.

(8) (a) Michael, D.; Mingos, P.; Baghurst, D. R. *Chem. Soc. Rev.* **1991**, *20*, 1−47. (b) Gerbec, J. A.; Magana, D.; Washington, A.; Strouse, G. F. *J. Am. Chem. Soc.* **2005**, *127*, 15791−15800.

(9) (a) Barthel-Rosa, L. P.; Gladysz, J. A. *Coord. Chem. Rev.* **1999**, *190-192*, 587−605. (b) Kataoka, H.; Lord, H. L.; Pawliszyn, J. J. *Chromatogr. A* **2000**, *880*, 35−62.

(10) Hessel, C. M.; Henderson, E. J.; Veinot, J. G. C. *Chem. Mater.* **2006**, *18*, 6139−6146.

(11) (a) Takagahara, T.; Takeda, K. *Phys. Rev. B: Condens. Matter Mater. Phys.* **1992**, *46*, 15578. (b) Allan, G.; Delerue, C.; Lannoo, M. *Phys. Rev. Lett.* **1996**, *76*, 2961. (c) Wilcoxon, J. P.; Samara, G. A.; Provencio, P. N. *Phys. Rev. B: Condens. Matter Mater. Phys.* **1999**, *60*, 2704.

(12) Purkait, T. K.; Iqbal, M.; Wahl, M. H.; Gottschling, K.; Gonzalez, C. M.; Islam, M. A.; Veinot, J. G. C. *J. Am. Chem. Soc.* **2014**, *136*, 17914−17917.

(13) (a) Zhao, K.; Li, J.; Wang, H. Z.; Zhuang, J. Q.; Yang, W. S. *J. Phys. Chem. C* **2007**, *111*, 5618−5621. (b) Kopainsky, B.; Qiu, P.;

DOI: 10.1021/jacs.5b08685
J. Am. Chem. Soc. 2015, 137, 14726−14732

Kaiser, W.; Sens, B.; Drexhage, K. H. *Appl. Phys. B: Photophys. Laser Chem.* **1982**, *29*, 15−18.
(14) (a) Kröger, N.; Deutzmann, R.; Sumper, M. *Science* **1999**, *286*, 1129−1132. (b) Noll, F.; Sumper, M.; Hampp, N. *Nano Lett.* **2002**, *2*, 91−95.
(15) Zhong, X. H.; Feng, Y. Y.; Knoll, W.; Han, M. Y. *J. Am. Chem. Soc.* **2003**, *125*, 13559−13563.
(16) (a) So, M. K.; Loening, A. M.; Gambhir, S. S.; Rao, J. H. *Nat. Protoc.* **2006**, *1*, 1160−1164. (b) Clapp, A. R.; Goldman, E. R.; Mattoussi, H. *Nat. Protoc.* **2006**, *1*, 1258−1267.
(17) Wu, X. Y.; Liu, H. J.; Liu, J. Q.; Haley, K. N.; Treadway, J. A.; Larson, J. P.; Ge, N. F.; Peale, F.; Bruchez, M. P. *Nat. Biotechnol.* **2002**, *21*, 41−46.
(18) Herndon, L. A.; Schmeissner, P. J.; Dudaronek, J. M.; Brown, P. A.; Listner, K. M.; Sakano, Y.; Paupard, M. C.; Hall, D. H.; Driscoll, M. *Nature* **2002**, *419*, 808−814.
(19) (a) Nelson, D. M.; Tréguer, P.; Brzezinski, M. A.; Leynaert, A.; Quéguiner, B. *Global Biogeochemical Cycles* **1995**, *9*, 359−372. (b) Armbrust, E. V.; Berges, J. A.; Bowler, C.; Green, B. R.; Martinez, D.; Putnam, N. H.; Zhou, S. G.; Allen, A. E.; Apt, K. E.; Bechner, M.; Brzezinski, M. A.; Chaal, B. K.; Chiovitti, A.; Davis, A. K.; Demarest, M. S.; Detter, J. C.; Glavina, T.; Goodstein, D.; Hadi, M. Z.; Hellsten, U.; Hildebrand, M.; Jenkins, B. D.; Jurka, J.; Kapitonov, V. V.; Kröger, N.; Lau, W. W. Y.; Lane, T. W.; Larimer, F. W.; Lippmeier, J. C.; Lucas, S.; Medina, M.; Montsant, A.; Obornik, M.; Parker, M. S.; Palenik, B.; Pazour, G. J.; Richardson, P. M.; Rynearson, T. A.; Saito, M. A.; Schwartz, D. C.; Thamatrakoln, K.; Valentin, K.; Vardi, A.; Wilkerson, F. P.; Rokhsar, D. S. *Science* **2004**, *306*, 79−86.
(20) (a) Fang, X. H.; Tan, W. H. *Acc. Chem. Res.* **2010**, *43*, 48−57. (b) Liu, S.; Zhang, X. Y.; Luo, W. X.; Wang, Z. X.; Guo, X. F.; Steigerwald, M. L.; Fang, X. H. *Angew. Chem., Int. Ed.* **2011**, *50*, 2496−2502. (c) Zhang, W.; Li, P.; Yang, F.; Hu, X. F.; Sun, C. Z.; Zhang, W.; Chen, D. Z.; Tang, B. *J. Am. Chem. Soc.* **2013**, *135*, 14956−14959. (d) Zhang, W.; Liu, W.; Li, P.; Xiao, H. B.; Wang, H.; Tang, B. *Angew. Chem., Int. Ed.* **2014**, *53*, 12489−12493. (e) Hong, G. S.; Diao, S.; Chang, J. L.; Antaris, A. L.; Chen, C. X.; Zhang, B.; Zhao, S.; Atochin, D. N.; Huang, P. L.; Andreasson, K. I.; Kuo, C. J.; Dai, H. J. *Nat. Photonics* **2014**, *8*, 723−730. (f) Hong, G. S.; Lee, J. C.; Robinson, J. T.; Raaz, U.; Xie, L. M.; Huang, N. F.; Cooke, J. P.; Dai, H. J. *Nat. Med.* **2012**, *18*, 1841−1846. (g) Tao, Z. M.; Hong, G. S.; Shinji, C.; Chen, C. X.; Diao, S.; Antaris, A. L.; Zhang, B.; Zou, Y. P.; Dai, H. J. *Angew. Chem., Int. Ed.* **2013**, *52*, 13002−13006.
(21) (a) Weyhenmeyer, G. A.; Peter, H.; Willén, E. *Freshwater Biol.* **2013**, *58*, 612−623. (b) Weyhenmeyer, G. A.; Broberg, N. *Aquat. Ecosyst. Health Manage.* **2014**, *17*, 341−348.
(22) Su, Y. Y.; Peng, F.; Jiang, Z. Y.; Zhong, Y. L.; Lu, Y. M.; Jiang, X. X.; Huang, Q.; Fan, C. H.; Lee, S. T.; He, Y. *Biomaterials* **2011**, *32*, 5855−5862.

DOI: 10.1021/jacs.5b08685
J. Am. Chem. Soc. 2015, 137, 14726−14732